Electronic Supplementary Material (ESI) for Dalton Transactions.

Electronic Supplementary Information

A New Barium Fluorooxoborate $BaB_5O_8F \cdot xH_2O$ with Large Birefringence and Wide UV Transparency Window

Chunmei Huang,[a,b,#] Guopeng Han [a,b,#], Hao Li,[a,b] Fangfang Zhang,[a,b,c,*] Zhihua Yang,[a,b,c] Shilie Pan[a,b,c*]

[a]CAS Key Laboratory of Functional Materials and Devices for Special Environments; Xinjiang Technical Institute of Physics & Chemistry, CAS; Xinjiang Key Laboratory of Electronic Information Materials and Devices, 40-1 South Beijing Road, Urumqi 830011, China.

[b]Center of Materials Science and Optoelectronics Engineering, University of Chinese Academy of Sciences, Beijing 100049, China.

[c]Fujian Institute of Innovation, Chinese Academy of Sciences, Fuzhou, 350002, China.

[#]These authors contributed equally to this work.

[*]Corresponding authors: ffzhang@ms.xjb.ac.cn, slpan@ms.xjb.ac.cn

Experimental Section

Synthesis. Single crystals of $BaB_5O_8F \cdot xH_2O$ were obtained by the solid-state reaction in a closed vacuum system. A mixture of B_2O_3 (0.522g, 7.498 mmol), NH_4F (0.200g, 5.399 mmol), and BaF_2 (0.439g, 2.448 mmol) was sealed into a silica glass tube (Φ10 mm × 150 mm), and the tube was flame-sealed under ~ 10^{-3} Pa to create a vacuum environment. Then, the tube was placed in a computer-controlled furnace, heated to 450 °C in 12 h, held at this temperature for 24 h, and then cooled to 30 °C at a rate of 2.5 °C/h. Millimeter-level blocky crystals were separated mechanically from the tube. In order to study the stability of the title compound against aqueous acids and bases, the following experiments were performed. The polycrystalline samples of the title compound were added into the aqueous solutions of hydrochloric acid and potassium hydroxide, respectively, with thoroughly stirring. It was shown that the samples in acids were dissolved and some floccule appeared in the solutions. In contrast, the polycrystalline samples in the potassium hydroxide aqueous solutions were not dissolved. Then the powder XRD of the precipitates was measured, and the result showed that the title compound and BaF_2 still existed.

Characterization.

Single-crystal XRD. The single-crystal XRD data were collected on a Bruker SMART APEX II 4K CCD diffractometer using Mo Kα radiation (λ = 0.71073 Å) at room temperature. Data integration, cell refinement and absorption corrections were carried out with the program SAINT.[1] The structure was solved by direct method and refined on F^2 by full-matrix least-squares technique using the program suite SHELXTL,[2] which was converged at R_1 = 0.0279, wR_2 = 0.0677, and S = 1.078, indicative of a correct absolute structure. The maximum and minimum residual electron densities ($\Delta\rho_{max,\ min}$) in different Fourier maps were 2.137 and − 0.670 e·Å^{-3}, respectively. The largest residual density is presumably attributed to a lattice water site with partial occupancy. This water site is at a distance of 2.95 Å from the Ba atom and refined to a site occupancy factor of 0.17, which is approximately equivalent to 0.17 water molecule per formula unit. The final cycles of least squares refinement are converged at R_1 =

0.0244, wR_2 = 0.0511, and S = 1.059, $\Delta\rho_{max,\ min}$ = 0.761 and 0.677 e·Å^{-3}. Solutions were checked for missed symmetry using PLATON.[3]

Elemental analysis. Elemental analysis was carried on clean single crystal surface with the aid of a field emission scanning electron microscope (SEM, SUPRA 55VP) equipped with an energy dispersive X-ray spectroscope (EDX, BRUKER x-flash-sdd-5010). The elemental analysis confirmed the structure model and verified the absence or presence of the Ba, B, F and O atoms (Figure S1).

Crystal data and structure refinement information are given in Table S1. The final refined atomic positions and isotropic thermal parameters are summarized in Table S2. Selected bond distances (Å) and angles (°) are listed in Table S3.

TG and DSC analyses were carried out on a simultaneous NETZSCH STA 449 F3 thermal analyzer instrument in a flowing N_2 atmosphere. The sample was placed in the Pt crucible, heated from 40 to 900 °C at a rate of 5 °C min^{-1}.

Infrared (IR) spectroscopy was measured on a Shimadzu IR Affinity-1 Fourier transform infrared spectrometer in the 400-4000 cm^{-1} range.

UV-vis-NIR diffuse-reflectance spectroscopy data were recorded at room temperature using a powder sample of $BaB_5O_8F{\cdot}xH_2O$ on a Shimadzu SolidSpec-3700DUV spectrophotometer.

Computational Methods. The first-principles calculations were performed by the plane-wave pseudopotential method implemented in the CASTEP package.[4] The exchange-correlation potential was calculated using Perdew-Burke-Ernzerhof (PBE) functional within the generalized gradient approximation (GGA) with the scheme.[5] To achieve energy convergence, the kinetic energy cutoff of 940 eV for $BaB_5O_8F{\cdot}xH_2O$ within normal-conserving pseudopotential (NCP) was adopted.[6] The Monkhorst-Pack *k*-point meshes in the Brillouin zone was set as 3 × 4 × 2 for $BaB_5O_8F{\cdot}xH_2O$.

Table S1. Crystal data and structure refinement for $BaB_5O_8F \cdot xH_2O$.

Empirical formula	$BaB_5O_8F \cdot xH_2O$ (x = 0.17)
Formula weight	341.39
Temperature	296.15 K
Crystal system, space group	Orthorhombic, *Pbca*
Unit cell dimensions	a = 11.399(3) Å
	b = 9.429(3) Å
	c = 13.467(4) Å
Volume	1447.4(7) Å^3
Z, Calculated density	8, 3.133 g·cm^{-3}
Absorption coefficient	5.527 mm^{-1}
F(000)	1245
Theta range for data collection	3.025 to 27.583 °
Limiting indices	$-14 \le h \le 14$, $-7 \le k \le 12$, $-15 \le l \le 17$
Reflections collected / unique	8352 / 1673 [R(int) = 0.0404]
Completeness to theta = 27.583 °	100.0 %
Data / restraints / parameters	1673 / 3 / 151
Goodness-of-fit on F^2	1.059
Final R indices [$F_o^2 > 2\sigma(F_o^2)$][a]	R_1 = 0.0244, wR_2 = 0.0511
R indices (all data)[a]	R_1 = 0.0329, wR_2 = 0.0551
Largest diff. peak and hole	0.761 and – 0.677 e·Å^{-3}

[a]$R_1 = \Sigma||F_o| - |F_c|| / \Sigma|F_o|$ and $wR_2 = [\Sigma w (F_o^2 - F_c^2)^2 / \Sigma w F_o^4]^{1/2}$ for $F_o^2 > 2\sigma(F_o^2)$

Table S2. Atomic coordinates (× 10^4), wyckoff positions, equivalent isotropic displacement parameters (Å^2 × 10^3) and bond valence sums (BVS) for $BaB_5O_8F{\cdot}xH_2O$. *U*(eq) is defined as one third of the trace of the orthogonalized U_{ij} tensor.

Atoms	Wyck.	S.O.F	*x*	*y*	*z*	*U*(eq)	BVS
Ba1	8c	1	4373(1)	1622(1)	3779(1)	11(1)	2.1
B1	8c	1	5303(4)	-1829(5)	3664(3)	8(1)	3.1
B2	8c	1	3370(4)	-1507(5)	4641(3)	8(1)	3.1
B3	8c	1	1503(4)	1844(5)	3241(3)	10(1)	3.0
B4	8c	1	7546(4)	2863(5)	3948(3)	10(1)	3.0
B5	8c	1	6840(4)	-351(5)	2822(3)	9(1)	3.0
O1	8c	1	5696(2)	-735(3)	2932(2)	12(1)	2.0
O2	8c	1	4564(2)	-1136(3)	4384(2)	10(1)	2.2
O3	8c	1	2170(2)	2604(3)	3892(2)	11(1)	2.2
O4	8c	1	6615(2)	2217(3)	4389(2)	11(1)	2.1
O5	8c	1	7151(2)	850(3)	2292(2)	11(1)	2.1
O6	8c	1	8675(2)	2555(3)	4177(2)	10(1)	2.0
O7	8c	1	7275(2)	3875(3)	3226(2)	11(1)	2.0
O8	8c	1	342(2)	2054(3)	3105(2)	10(1)	2.0
F1	8c	1	2724(2)	-223(3)	4715(2)	14(1)	0.9
O9	8c	0.1677	4840(19)	4530(20)	4472(17)	31(5)	
H9A	8c	0.1677	4800(300)	5320(190)	4800(200)	47	
H9B	8c	0.1677	5430(180)	4100(200)	4700(200)	47	

Table S3. Selected bond lengths (Å) and angles (°) for $BaB_5O_8F \cdot xH_2O$.

Ba1-O3	2.682(3)	B2-F1	1.421(5)
Ba1-O2	2.735(3)	B2-O3#6	1.450(5)
Ba1-O4	2.743(3)	B2-O2	1.447(5)
Ba1-O2#1	2.792(3)	B2-O4#1	1.468(5)
Ba1-O8#2	2.796(3)	B3-O8	1.354(5)
Ba1-F1	2.855(2)	B3-O3	1.362(5)
Ba1-O(1)	2.918(3)	B3-O5#2	1.393(5)
Ba1-O6#3	2.969(3)	B4-O6	1.354(5)
Ba1-O5#4	3.005(3)	B4-O4	1.360(5)
Ba1-O9	2.950(2)	B1-O1	1.496(5)
B1-O2	1.442(5)	B4-O7	1.398(5)
B1-O6#5	1.475(5)	B5-O7#5	1.360(5)
B1-O8#6	1.487(5)	B5-O1	1.361(5)
O(9)-H(9A)	0.85(2)	B5-O5	1.384(5)
O(9)-H(9B)	0.85(2)		
O2-B1-O6#5	109.0(3)	O2-B2-O4#1	108.2(3)
O2-B1-O8#6	111.9(3)	O8-B3-O3	123.7(4)
O6#5-B1-O8#6	110.4(3)	O8-B3-O5#2	123.3(4)
O2-B1-O1	107.8(3)	O3-B3-O5#2	112.9(4)
O6#5-B1-O1	110.1(3)	O6-B4-O4	123.0(4)
O8#6-B1-O1	107.6(3)	O6-B4-O7	121.0(4)
F1-B2-O3#6	108.8(3)	O4-B4-O7	115.9(4)
F1-B2-O2	107.4(3)	O7#5-B5-O1	121.7(4)
O3#6-B2-O2	111.9(3)	O7#5-B5-O5	117.0(4)
F1-B2-O4#1	109.4(3)	O1-B5-O5	121.3(4)
O3#6-B2-O4#1	111.1(3)	H(9B)-O(9)-H(9A)	105(3)

Symmetry transformations used to generate equivalent atoms:

#1 −x+1, −y, −z+1 #2 x−1/2, y, −z+1/2 #3 x−1/2, −y+1/2, −z+1

#4 x−1/2, y, −z+1/2 #5 −x+3/2, y−1/2, z #6 −x+1/2, y−1/2, z

#7 −x+1/2, −y+1, −z+1 #8 −x+1/2, y+1/2, z #9 −x+3/2, y+1/2, z

#10 x+1/2, −y+1/2, −z+1

Table S4. Assignment of the absorption bands observed in the IR spectrum for $BaB_5O_8F \cdot xH_2O$.

Absorption bands (cm^{-1})	Assignment
3323	asymmetric stretching of H-O
1632	the bending of group H-O-H
1399, 1303	asymmetric stretching of B-O in the $[BO3]^{3-}$
1083, 1026	asymmetric stretching of B-O in the $[BO_4]^{5-}$
918	symmetric stretching of B-O in the $[BO_3]^{3-}$
870, 804	symmetric out of phase stretching of the B-F bond
752	symmetric stretching of B-O in the $[BO_4]^{5-}$
623, 576	out-of-plane bending modes of $[BO_3]^{3-}$
487	out-of-plane bending modes of $[BO_4]^{5-}$

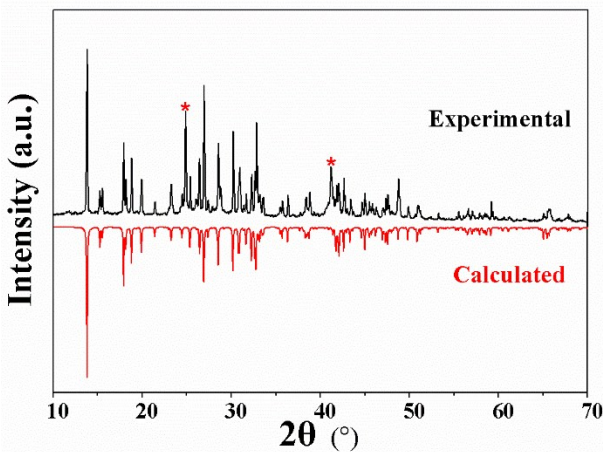

Figure S1. X-ray diffraction patterns of $BaB_5O_8F{\cdot}xH_2O$. The impurity phases BaF_2 have been marked in red "*".

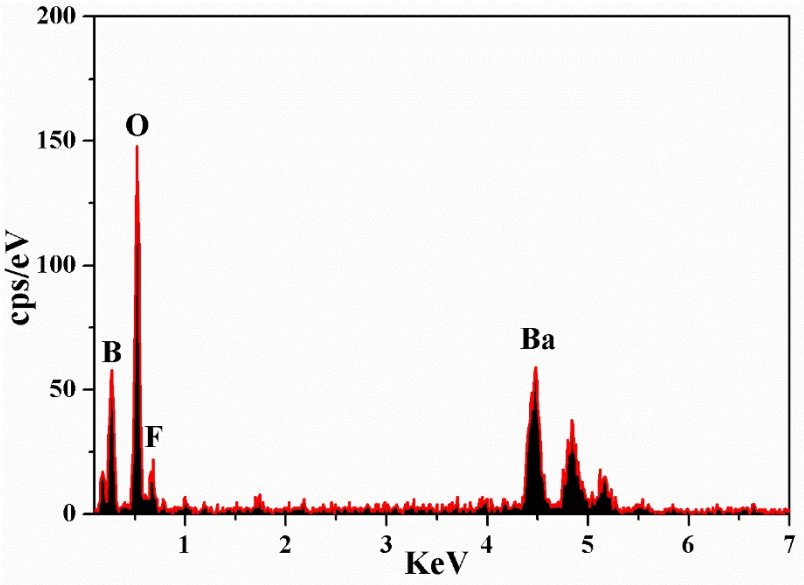

Figure S2. Energy dispersive X-ray (EDX) spectroscopy of $BaB_5O_8F \cdot xH_2O$. EDX spectrum was performed to verify the absence or presence of the F and O atoms because the X-ray diffraction cannot distinguish the two atoms. The EDX spectrum shows that the F atoms indeed exist in the crystal structure.

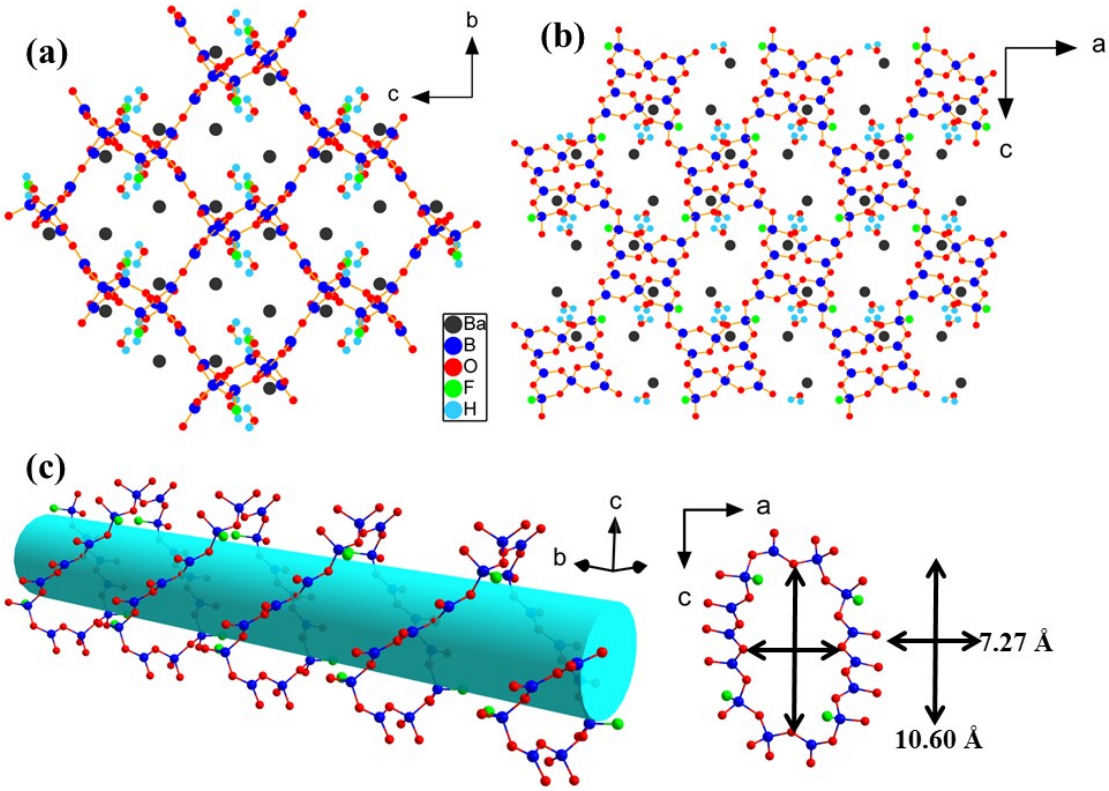

Figure S3. Crystal structure of $BaB_5O_8F{\cdot}xH_2O$. Projective views of the crystal structure along the *a* axis (a) and the *b* axis (b); (c) Large pseudo-channel of $BaB_5O_8F{\cdot}xH_2O$.

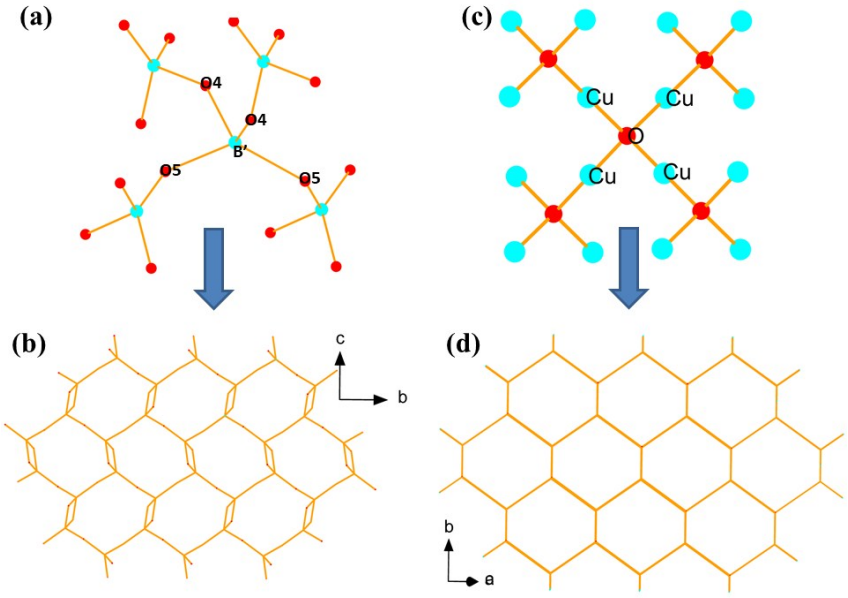

Figure S4. Coordination environment of the pseudo-tetrahedral $B'O_4$ by considering the FBB as a pseudo-tetrahedral basic building unit since the four terminal oxygen atoms O4 and O5 show an arrangement like a distorted tetrahedron centred by B' (a four-coordinate node) (a); One of the topologically interpenetrating B-O tetrahedral networks in the title compound (b); Coordination environment of the tetrahedral OCu_4 in Cu_2O (c); One of the topologically interpenetrating Cu-O tetrahedral networks in Cu_2O (d).

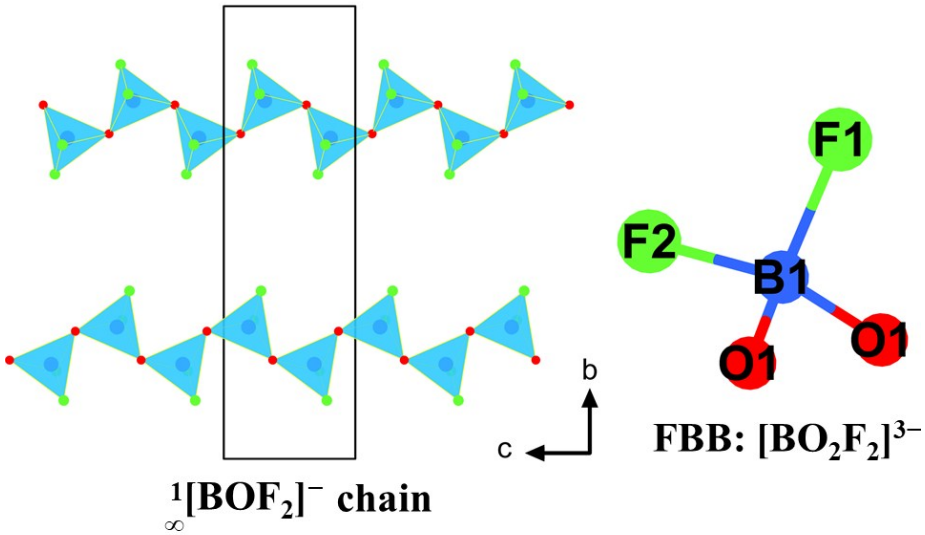

Figure S5. 1D chains $^{1}_{\infty}[BOF2]^{-}$ of $BaBOF_3$.[7]

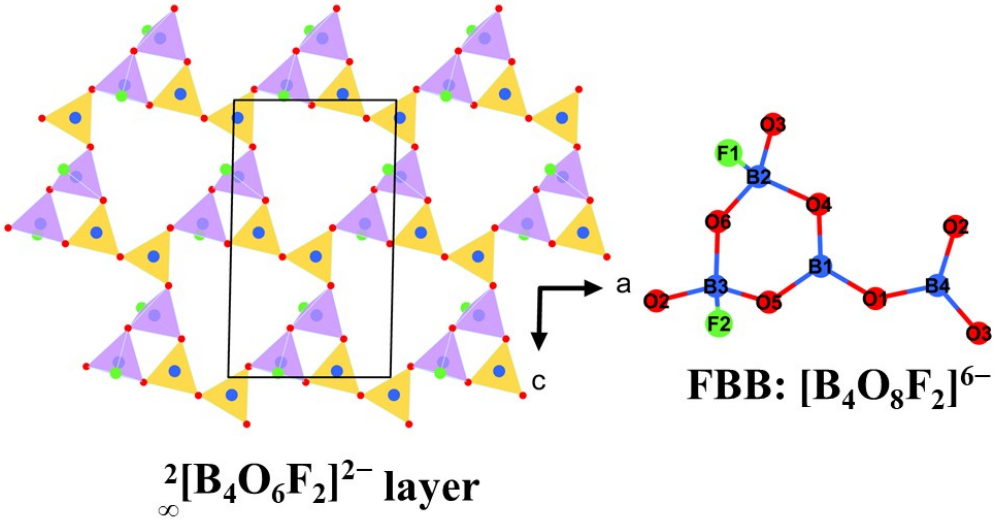

Figure S6. 2D layers $^2_\infty$[B4O6F2]2 - in the *ac* plane of $BaB_4O_6F_2$.[8]

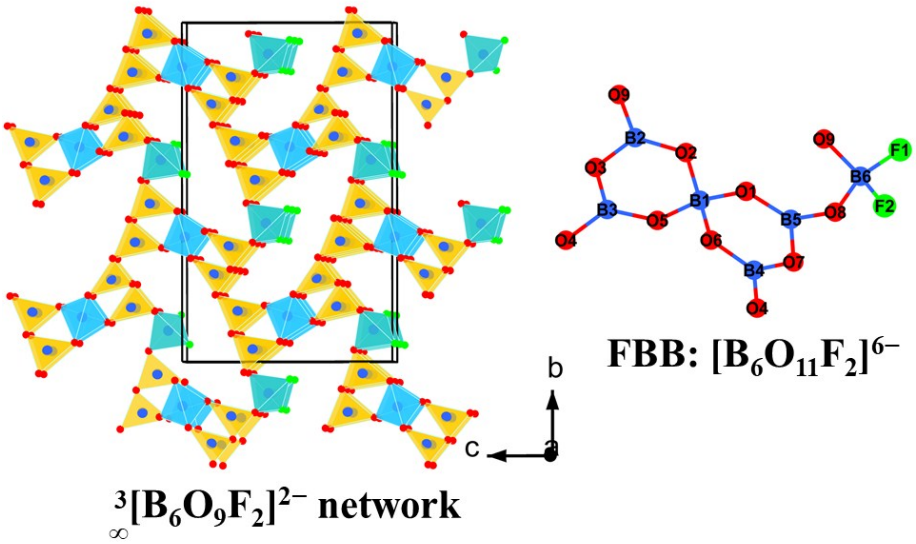

Figure S7. 3D network $^{3}_{\infty}$[B6O9F2]2 - of $Li_2B_6O_9F_2$.[9]

References

1 SAINT, *Version 7.60A,* Bruker Analytical X-ray Instruments, Inc., Madison, WI, 2008.

2 G. M. Sheldrick, *SHELXTL, version 6.12; Bruker Analytical X-ray Instruments, Inc.: Madison, WI,* 2001.

3 A. L. Spek, *J. Appl. Crystallogr.,* 2003, **36**, 7.

4 S. J. Clark, M. D. Segall, C. J. Pickard, P. J. Hasnip, M. J. Probert, K. Refson and M. C. Payne, *Z. Anorg. Allg. Chem.,* 2005, **220**, 567.

5 J. P. Perdew, K. Burke and M. Ernzerhof, *Phys. Rev. Lett.,* 1996, **77**, 3865.

6 (a) A. M. Rappe, K. M. Rabe, E. Kaxiras and J. D. Joannopoulos, *Phys. Rev. B,* 1990, **41**, 1227; (b) J. S. Lin, A. Qteish, M. C. Payne and V. Heine, *Phys. Rev. B,* 1993, **47**, 4174.

7 D. Q. Jiang, Y. Wang, H. Li, Z. H. Yang and S. L. Pan, *Dalton Trans*., 2018, **47**, 5157.

8 S. G. Jantz, F. Pielnhofer, L. van Wüllen, R. Weihrich, M. J. Schäfer and H. A. Höppe, *Chem. Eur. J*., 2018, **24**, 443.

9 T. Pilz and M. Jansen, *Z. Anorg. Allg. Chem.,* 2011, **637**, 2148.